Limnol. Oceanogr., 52(4), 2007, 1367–1379

Biogas (CO_2, O_2, dimethylsulfide) dynamics in spring Antarctic fast ice

Bruno Delille[1]
Unité d'Océanographie Chimique, Interfacultary Centre for Marine Research, Université de Liège, Allée du 6 Août, 17, 4000 Liège, Belgium

Bruno Jourdain[2]
Laboratoire de Glaciologie et Géophysique de l'Environnement, CNRS-UMR 5183, 54 rue Molière, 38402 St Martin d'Hères, France

Alberto V. Borges
Unité d'Océanographie Chimique, Interfacultary Centre for Marine Research, Université de Liège, Allée du 6 Août, 17, 4000 Liège, Belgium

Jean-Louis Tison
Glaciology Unit, Department of Earth and Environmental Science, Université Libre de Bruxelles, CP 160/03, 50 Ave. F.D. Roosevelt, 1050 Bruxelles, Belgium

Daniel Delille
Observatoire Océanologique de Banyuls, Université Pierre et Marie Curie, URA CNRS 117, Laboratoire Arago, 66650 Banyuls-sur-mer, France

Abstract

We studied the temporal variations of CO_2, O_2, and dimethylsulfide (DMS) concentrations within three environments (sea-ice brine, platelet ice-like layer, and underlying water) in the coastal area of Adélie Land, Antarctica, during spring 1999 before ice breakup. Temporal changes were different among the three environments, while similar temporal trends were observed within each environment at all stations. The underlying water was always undersaturated in O_2 (around 85%) and oversaturated in CO_2 at the deepest stations. O_2 concentrations increased in sea-ice brine as it melted, reaching oversaturation up to 160% due to the primary production by the sea-ice algae community (chlorophyll *a* in the bottom ice reached concentrations up to 160 μg L^{-1} of bulk ice). In parallel, DMS concentrations increased up to 60 nmol L^{-1} within sea-ice brine and the platelet ice-like layer. High biological activity consumed CO_2 and promoted the decrease of partial pressure of CO_2 (pCO_2). In addition, melting of pure ice crystals and calcium carbonate ($CaCO_3$) dissolution promoted the shift from a state of CO_2 oversaturation to a state of marked CO_2 undersaturation ($pCO_2 < 30$ dPa). On the whole, our results suggest that late spring land fast sea ice can potentially act as a sink of CO_2 and a source of DMS for the neighbouring environments, i.e., the underlying water or/and the atmosphere.

Sea ice covers about 7% of Earth's surface at its maximum seasonal extent, representing one of the largest biomes on the planet. For decades, sea ice was assumed to be an impermeable and inert barrier for air-sea exchanges of CO_2, and global climate models did not include CO_2 exchanges between this compartment and the atmosphere. However, there is a growing body of evidence that sea ice exchanges CO_2 with the atmosphere. While estimating permeation constants of sulfur hexafluoride (SF_6) and CO_2 within sea ice, Gosink et al. (1976) stressed that sea ice is a permeable medium for gases. These authors suggested that gas migration through sea ice could be an important factor in winter ocean-atmosphere exchange at sea-ice surface temperature above -10°C. More recently, uptake of atmospheric CO_2 over sea-ice cover has been reported (Semiletov et al. 2004; Delille 2006; Zemmelink et al. 2006) supporting the need to further investigate pCO_2 dynamics in the sea-ice realm and related CO_2 fluxes.

Very few studies have been carried out on the dynamics of the carbonate system within natural sea ice. They have generally been aimed at investigating $CaCO_3$ precipitation or dissolution (Gleitz et al. 1995), or they have focused on measurements of dissolved inorganic carbon (DIC) and total alkalinity (TA) (Anderson and Jones, 1985; Rysgaard et al. 2007) rather than on pCO_2. As pointed out by

[1] Corresponding author (Bruno.Delille@ulg.ac.be).
[2] Present address: Laboratoire Chimie et Environnement, Université de Provence, Case 29, 3, Place Victor Hugo, 13331 Marseille Cedex 3, France.

Acknowledgments

The authors thank P. David and the other members of the Institut Paul-Emile Victor at the Dumont D'Urville Station during November and December 1999. We are indebted to Tim Papakyriakou and one anonymous reviewer for comments that significantly improved the manuscript. This research was supported by the Belgian Science Policy (contract A4/DD/B14, EV/7/12E, SD/CA/03A, OA/00/025), the Institut Paul-Emile Victor, and the Fonds de la Recherche Scientifique, where A.V.B. is a research associate. This is Interfacultary Centre for Marine Research contribution 107.

Rysgaard et al. (2007), precipitation of carbonate minerals within sea ice could drive significant CO_2 uptake, but such a phenomenon remains to be investigated and has not been systematically observed (Gleitz et al. 1995; Thomas and Deickmann 2002). The observations of Papadimitriou et al. (2004) and Rysgaard et al. (2007) suggest that during sea-ice formation in fall and winter, carbonate precipitation can occur within sea ice. According to Rysgaard et al. (2007), a significant fraction of CO_2 generated as a by-product of carbonate precipitation appears to be removed during brine expulsion and is partly exported below the pycnocline during deep-water formation. While CO_2-enriched brines are expelled from the ice, carbonate minerals could remain trapped in the brine tubes and channels until spring and summer, when they would dissolve within the sea ice or in the underlying water. Such dissolution consumes CO_2 and therefore acts as a sink for atmospheric CO_2 (Rysgaard et al. 2007). Other processes can potentially act as sinks of CO_2. First, sea ice hosts algae communities, the primary production of which has been estimated to account for 10% to 28% of the total production of the Southern Ocean (e.g., Arrigo and Thomas 2004). Second, during sea-ice growth, most of the impurities (solutes, gases, particulate matter) are expelled from the pure ice crystals at the ice-water interface (Killawee et al. 1998). The CO_2 rejected into the boundary layer will either diffuse or be convectively driven downward into the underlying water, removing CO_2 from the surface water. During spring, melting of CO_2-depleted sea ice would decrease pCO_2 of surface waters. Such a mechanism would act as a sink for atmospheric CO_2. On the whole, spring sea ice appears to act as a CO_2 sink that may be significant in the budget of CO_2 fluxes in the Southern Ocean (Delille 2006; Zemmelink et al. 2006).

Antarctic sea ice has been shown to contain large amounts of dimethylsulphoniopropionate (DMSP) (Turner et al. 1995; Trevena et al. 2003; Gambaro et al. 2004), which is a precursor of dimethylsulfide (DMS), another climatically active gas. Marine DMS emissions are involved in climate regulation because atmospheric oxidation products of DMS act as condensation nuclei and therefore directly (as aerosols) and indirectly affect the radiative properties of the atmosphere. DMS is a byproduct of DMSP, which is synthesized by a few classes of marine micro- and macroalgae and some higher plants (e.g., Stefels 2000). DMS is produced by enzymatic cleavage of released DMSP by bacteria and algae. The physiological role of DMSP in phytoplankton and sea-ice algae is poorly understood (Stefels 2000). It has been suggested that DMSP can act as an active osmolyte and cryoprotectant at the same time (Dickson and Kirst 1986), an antioxidant that protects cells during oxidative stress conditions (ultraviolet radiation, CO_2 and/or Fe limitation, high Cu^{2+} and H_2O_2 concentration; Sunda et al. 2002), a grazing-activated chemical defense precursor or a "trash-can" for reduced compounds and excess energy (Stefels 2000). DMSP release by the cell occurs during algal growth but significantly increases during cell senescence or as a consequence of zooplankton grazing, bacterial activity, and viral lysis. During sea-ice melting, DMSP and DMS released from the ice can accumulate in surface waters and lead to the occurrence of DMS concentration pulses and hot-spots (Kirst et al. 1991; Levasseur et al. 1994; Trevena and Jones 2006). Zemmelink et al. (2005) reported that the stratification due to sea-ice melting fosters the production of DMSP and DMS in sea ice in such amounts that the resulting emission could contribute significantly to the yearly DMS flux from the Southern Ocean to the atmosphere. Hence, sea ice–related processes appear to act as a source of DMS, which could be significant in the budget of DMS fluxes to the atmosphere in the Southern Ocean.

To our best knowledge, there are very few studies on DMS and CO_2 dynamics within natural sea ice. Turner et al. (1995) investigated DMS and DMSP in the Bellingshausen Sea and Drake Passage, Trevena and Jones (2006) investigated DMS in Prydz Bay, and Kirst et al. (1991) and Gambaro et al. (2004) carried out measurements of DMSP in the Weddell Sea and in Terra Nova Bay, respectively. Even fewer measurements of CO_2 are available: Gleitz et al. (1995) and Delille (2006) investigated CO_2 dynamics in the Weddell Sea and Eastern Antarctica, respectively, while Rysgaard et al. (2007) focused on Arctic sea ice. Here, we present and discuss the first joint temporal survey of DMS, pCO_2, and O_2 concentrations within sea-ice brine and the underlying water.

Material and methods

Site and sampling—The study was carried out from 10 Nov to 16 Dec 99 just before the sea-ice cover breakup in the Géologie Archipelago, Adélie Land, Antarctica (66°40′S, 140°01′E). The area is covered from March-April to December by a homogeneous and solid layer of land-fast ice. Samples were collected at four contrasting stations along a south-north cross-shore transect (Fig. 1). Stations A to C were located in the shallow area close to the Dumont D'Urville Station, Astrolabe Glacier, and grounding line of the Antarctic continent, and sta. D was located 3.8 km off the coast. Bottom depth increased from sta. A to sta. D, and the four stations experienced various snow and ice thicknesses (Table 1) and sheltering conditions; sta. A was located in a small and well-sheltered cove, and sta. D was located in an open area.

At each station, all samples were collected within an area of about 40 m^2 in order to minimize bias from spatial heterogeneity. Ice brine was sampled by drilling sackholes to a depth of 50 cm using a 10-cm internal-diameter ice corer. The brine from adjacent brine channels and pockets was allowed to seep into the sackhole for 10–15 min before collection with the hole covered with a plastic lid, reportedly the best current method to sample brines for chemical studies (Papadimitriou et al. 2004). Brine for gas measurements was sampled by gently filling a 60-mL syringe and then transferring it to storage borosilicate bottles. One core was sampled for chlorophyll *a* (Chl *a*) and stored in a plastic bag. The bottom 10 cm of the core was cut and thawed in the dark. After drilling the ice cover, a loose matrix of water and platelet ice-like material, and underlying water were collected at a depth of 0 m and 1 m,

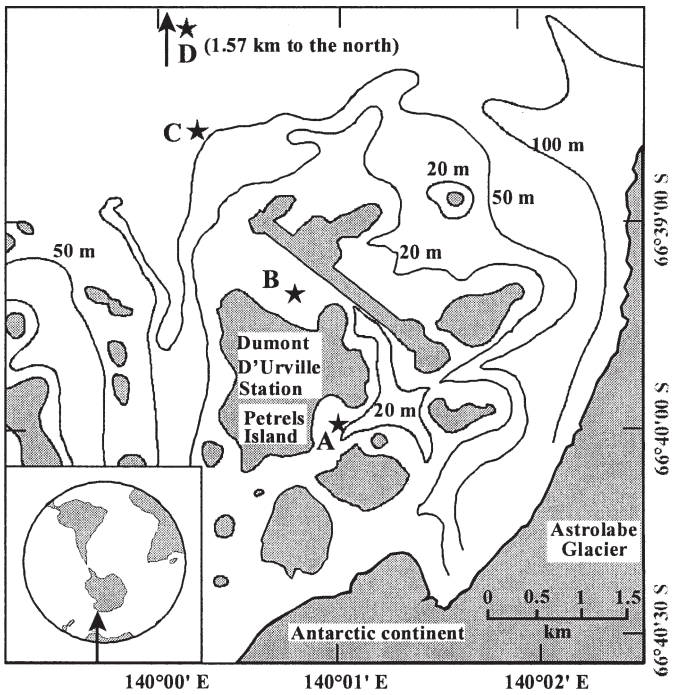

Fig. 1. Location of the stations and bottom topography in the vicinity of the French research station of Dumont D'Urville, located on Petrels Island, Adélie Land, Antarctica.

respectively, with a 1.5-liter borosilicate collecting bottle adapted with tubes to allow gentle filling and minimize bubbles formation. Underlying water and the liquid phase of the platelet ice-like matrix were gently transferred with a syringe from the collection bottle to storage borosilicate bottles without delay. Care was taken to avoid degassing and freezing during sampling and transportation to the laboratory.

Chlorophyll—Chl *a* samples were filtered by gentle vacuum filtration of 0.5 to 1 liters of sample through Whatman® GF/F glass-fiber filters. The measurements of Chl *a* were carried out following the recommendations of Arar and Collins (1997) with a Turner Designs® TD 700 fluorometer.

Dissolved inorganic carbon—DIC and pCO_2 were calculated from pH and TA measurements. The pH was measured using commercial combination electrodes (Ross type, Orion) calibrated on the total hydrogen ion scale using TRIS (2-amino-2-hydroxymethyl-1,3-propanediol) and AMP (2-aminopyridine) buffers prepared at salinities of 30, 35, 40, and 80, according to the formulations proposed by the DOE (1994). The pH measurements were carried out as soon as possible after return to the laboratory (typically less than 2 h after sampling), and samples were maintained at low yet nonfreezing temperature (typically between 0°C and 4°C) until measurement. The pH electrode was calibrated at temperatures ranging from 1°C to 3°C, at salinities of 30, 35, 40, and 80. The accuracy of pH measurements was ±0.01 pH units. Samples for TA measurements were filtered on GF/F glass filters within 3 h after return to the laboratory. TA was measured at the laboratory temperature within one day after sampling using the classical Gran electrotitration. The accuracy of measurements was ±4 μmol kg^{-1}. The CO_2 speciation was calculated from pH and TA measurements with the CO_2 acidity constants of Mehrbach et al. (1973) refitted by Dickson and Millero (1987) and other constants advocated by the DOE (1994). We assumed a conservative behaviour of CO_2 dissociation constants at subzero temperature. Indeed, Millero et al. (2002) reported that the CO_2 acidity constants of Mehrbach et al. (1973) refitted by Dickson and Millero (1987) were valid for a large range of temperature, from −1.6°C to 38°C. Furthermore, Marion (2001) showed that measurements of carbonate mineral solubilities for subzero temperatures (down to −21.6°C) fit with the prediction derived from the four important equilibrium constants of the aqueous carbonate system determined only for positive temperatures, namely, the first (K_1) and second (K_2) dissociation constants for carbonic acid, the Henry's Law constant for CO_2 (K_H), and the dissociation constant for water (K_W). This suggests that thermodynamic constants relevant for the carbonate system can be assumed to be valid at subzero temperatures. The pCO_2 values computed from pH and TA measurements were compared with direct pCO_2 measurements carried out using the conventional equilibration method for underway pCO_2 measurement (DOE, 1994) adapted for use in the field for pCO_2 measurements of brine (Delille 2006). The comparison was performed during the ISPOL cruise (Nov 2004–Jan 2005) in the western Weddell Sea, and it showed that indirect and direct pCO_2 measurements are consistent within ±10 dPa in underlying seawater and ±25 dPa in brine (Fig. 2).

Salinity was determined with a Guildline-Autosal induction salinometer with an accuracy of ±0.003. Samples above a salinity of 42 were diluted with deionized water prior to measurement.

Oxygen—Dissolved oxygen was measured with the Winkler method. Winkler reagents were added to the biological oxygen demand (BOD) bottle in the field just after sampling. Samples were maintained in the dark at positive temperature. Titration was performed within 24 h using a potentiometric end-point determination, with an estimated accuracy of ±2 μmol kg^{-1} (±0.8% of saturation level). Taking into account gas exchanges during filling of

Table 1. Position of stations A to D, approximate bottom depth, and ranges of snow and ice thickness.

Station	Position	Bottom depth (m)	Ice thickness (cm)	Snow thickness (cm)
A	66°39′58″S, 140°01′08″E	<10	168–176	0
B	66°39′38″S, 140°01′43″E	<20	158–171	0–1
C	66°39′28″S, 139°59′54″E	~50	133–153	0–2
D	66°38′09″S, 140°00′03″E	~200	112–113	20

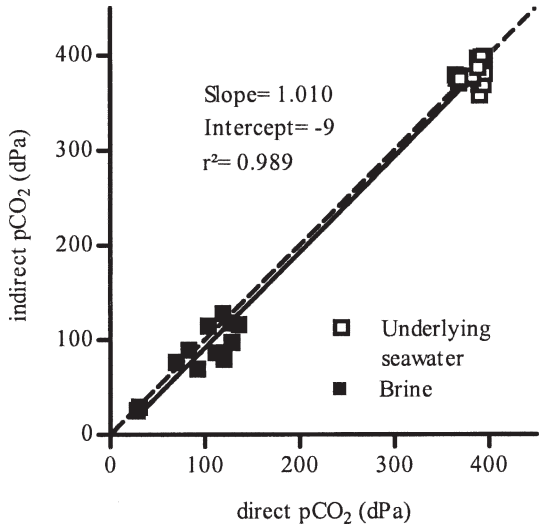

Fig. 2. Comparison of direct partial pressure of CO_2 (pCO_2) measurements and pCO_2 computed from pH and total alkalinity measurements (indirect pCO_2) carried out during the ISPOL cruise in the western Weddell Sea between Nov 2005 and Jan 2006. Open and filled squares correspond to underlying water and brine, respectively, while solid and dashed lines correspond to linear regression and 1 : 1 lines, respectively.

the sackhole, the estimated accuracy was ± 5 μmol kg^{-1} for brine measurements.

Dimethylsulfide—Dissolved DMS was sampled by flushing seawater or brines through a glass-fiber filter (Whatman GF/F, Ø47 mm) into 20-mL polyethylene vials that were completely filled and stored at 4°C to prevent DMS loss prior to analysis. DMS analyses were performed in the field within 4 h after sampling, using a gas chromatograph equipped with a flame photometric detector (HP 6890, 393 nm). A few milliliters of seawater were introduced into a glass device where DMS was degassed by a helium stream at a flow rate of 180 mL min^{-1}. DMS was then cryogenically trapped at −60°C on a Tenax GC 80 loaded tube maintained in a bath of ethanol cooled by a Cryocool CC100 device. DMS was subsequently transferred to the gas chromatograph by thermal desorption of the Tenax trap (boiling water) as detailed by Nguyen et al. (1990). Working chromatographic conditions were: an oven temperature of 95°C, a detector temperature of 200°C, and a flow rate at the flame of 30 mL min^{-1} of helium (carrier gas), 80 mL min^{-1} of air, and 55 mL min^{-1} of hydrogen. Calibrations were performed just before analysis using a permeation tube (VICI Metronics) placed in a bath thermostated at 30°C. This tube was calibrated against other permeation tubes used as reference for the monitoring of atmospheric DMS at Amsterdam Island and was found to produce 1.18 ng of DMS per min, with no detectable shift during one year. Calibration range was typically from 1.18 to 3.54 ng of DMS. The detection limit was close to 0.2 ng of DMS, leading to a DMS detection limit under 0.3 nmol L^{-1} for 10 mL of seawater. Taking into account gas exchange during filling of the sackhole, the estimated accuracy was ± 1 nmol L^{-1} for brine measurements.

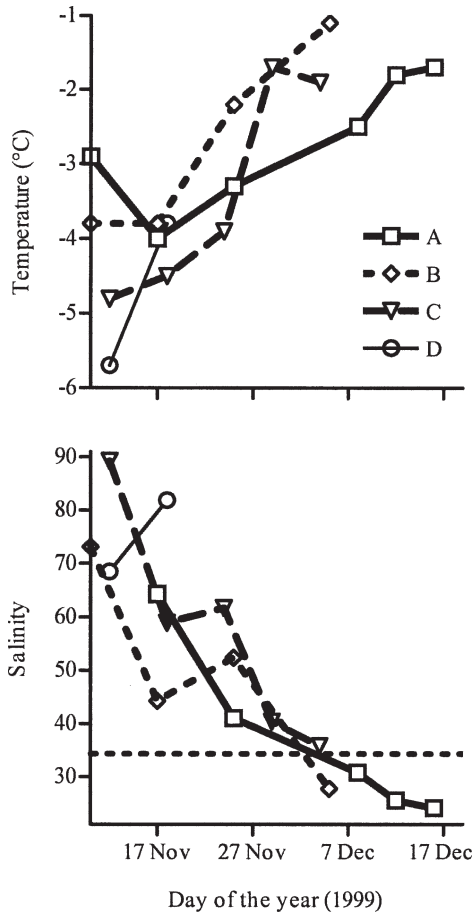

Fig. 3. Temporal variation of temperature and salinity of brines. Horizontal dotted line shows mean salinity of the underlying water.

Results

Sea-ice conditions—Sea ice broke up progressively over the course of the survey. At the start of the experiment, open water was found at ~10–20 km off the coast. Strong katabatic wind took place from 22 Nov to 25 Nov 99 and promoted offshore ice breakup that prevented further monitoring of sta. D; after that, several strong wind and ice breakup events, detailed by Riaux-Gobin et al. (2005), led to the disappearance of stations B and C, while sta. A remained throughout the survey. In order to investigate the evolution of pCO_2 after ice breakup, surface water at the location of stations B, C, and D was sampled on 16 Dec 99.

Temperature and salinity of the ice brines—In the course of the survey, brine temperature increased steadily at all stations, ranging from −5.7°C at sta. D to −1.1°C at sta. B (Fig. 3). As a consequence, ice crystals melted progressively, and salinity of brines drastically decreased from 89.2 at sta. C down to 24 at sta. A (Fig. 3). By early December, salinity of brines at stations A and B was lower than the

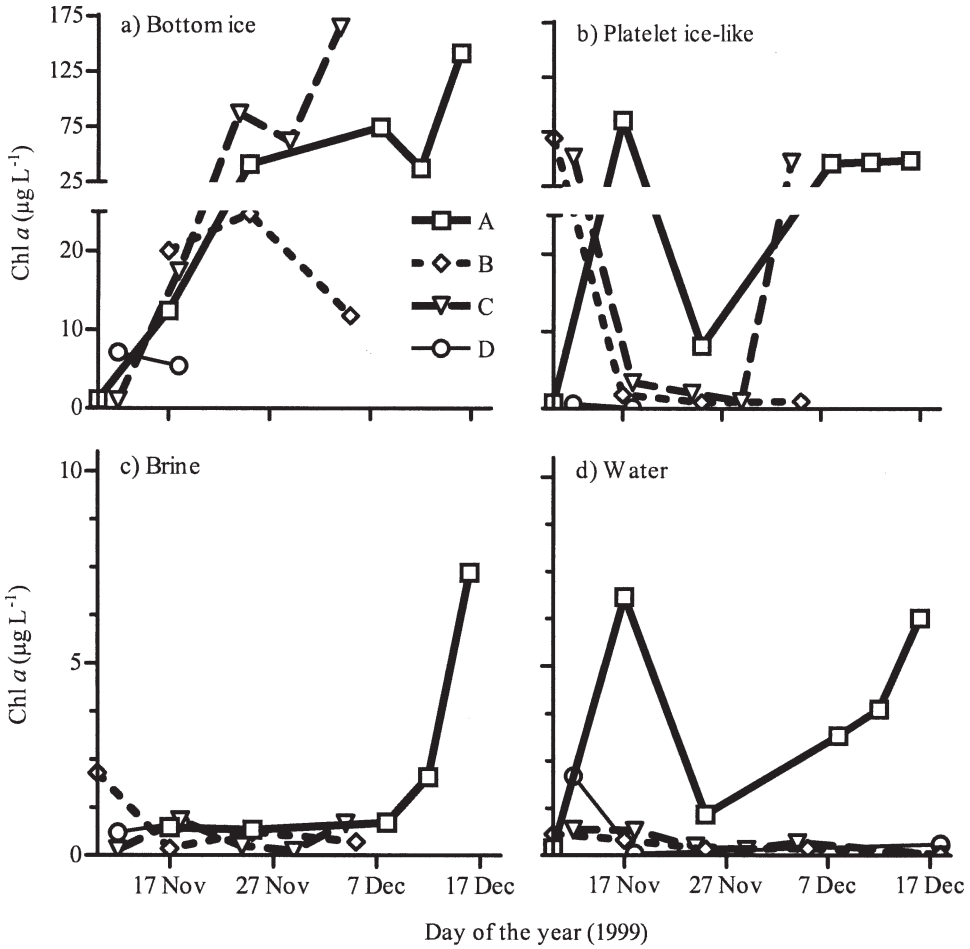

Fig. 4. Temporal variation of chlorophyll *a* concentration within (a) bottom ice, (b) platelet ice-like layer, (c) brines, and (d) underlying water at stations A, B, C, and D.

salinity of underlying seawater, which ranged from 34.3 to 35.0 (data not shown).

Chlorophyll a—Chl *a* concentration within the bottom sea ice increased drastically at stations A, B, and C (Fig. 4), ranging from 1.0 μg L^{-1} up to 164.0 μg L^{-1} of bulk ice at sta. A, which is in agreement with previous observations by Fiala et al. (2006). In contrast, Chl *a* concentration within brines remained below 2.0 μg L^{-1}, except during the last days of the survey at sta. A. Chl *a* concentration values in the platelet-like ice layer exhibited high temporal and spatial variability, ranging from 0.2 μg L^{-1} to 85.0 μg L^{-1} of bulk ice. The lowest Chl *a* concentration values were observed in the underlying water (typically $<$1.0 μg L^{-1}), with the exception of sta. A, where Chl *a* concentration mimicked the pattern observed in the platelet ice, although at a lower magnitude (Chl *a* concentration reached a maximum value of 6.8 μg L^{-1}).

Oxygen—Underlying water was undersaturated in O_2 throughout the survey, as previously reported in the Weddell Sea (Hoppema et al. 1995). O_2 saturation level ($\%O_2$) ranged from 83% to 91% (Fig. 5) and slightly increased from 25 Nov onward. In contrast, platelet ice exhibited a drastic increase of $\%O_2$, from a slight undersaturation similar to the one in the underlying water, to a marked oversaturation up to 148% at sta. C. Before ice breakup, $\%O_2$ at stations A, B, and C converged toward a value of 130%. $\%O_2$ in brines showed high temporal and spatial variability, with values ranging from 110% to 163%.

The pCO_2 and carbonate system—The pCO_2 of the underlying water ranged between 310 dPa and 460 dPa at stations A and B, while at stations C and D, pCO_2 ranged from the atmospheric equilibrium (about 370 dPa) to a slight oversaturation up to 395 dPa (Fig. 5). At stations A, B, and C, pCO_2 decreased steadily to reach a minimum before ice breakup, then increased rapidly to reach a maximum after breakup. The pCO_2 values in the platelet ice-like layer showed high spatial and temporal heterogeneity, but tended to decrease to reach values down to 65 dPa before ice breakup. Stations A, B, and C brines exhibited a conspicuous and similar decrease of CO_2 from an oversaturation, with pCO_2 values ranging from 400 dPa to 420 dPa, to a marked CO_2 undersaturation (pCO_2 values below 30 dPa).

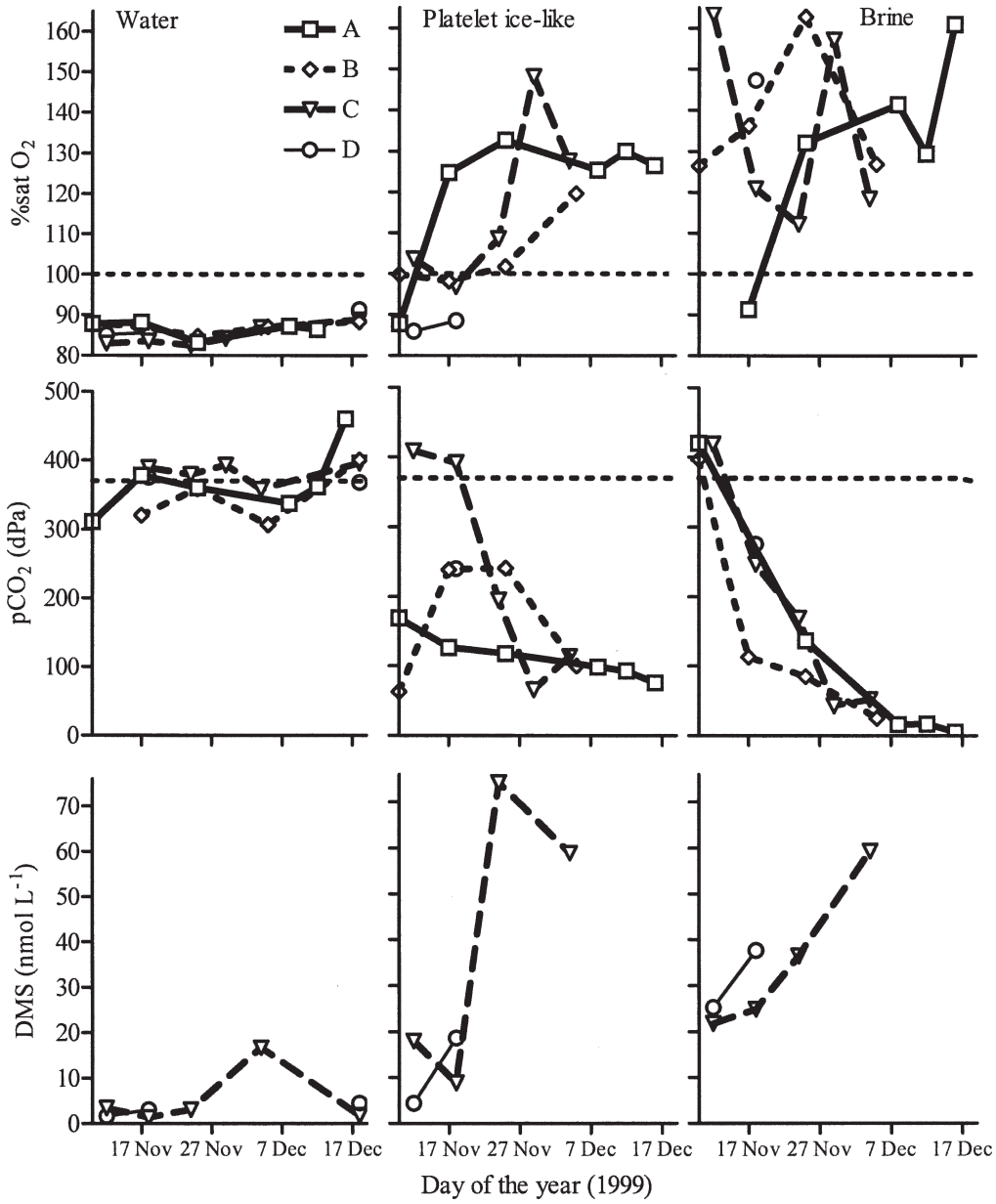

Fig. 5. Temporal variation of oxygen saturation level ($\%O_2$), partial pressure of CO_2 (pCO_2), and dimethylsulfide (DMS) concentration within the underlying water, platelet ice-like layer, and brines at stations, A, B, C, and D. Horizontal dotted lines correspond to O_2 and CO_2 saturation levels.

The pH (total scale) ranged from 8.04 to 8.15 in the underlying seawater, while brine exhibited pH values that ranged from 8.38 up to 9.42 (Fig. 6). DIC, normalized at a salinity of 35 (DIC_{35}), mimicked the overall decrease of pCO_2 within the platelet ice-like layer and brines (Fig. 6). TA, normalized at salinity of 35 (TA_{35}), slightly decreased in the underlying layer, while it exhibited a slight increase within brines at stations A and B during the first part of the experiment. This increase was enhanced at sta. C, where, similar to sta. D, TA_{35} values in the brines at the start of the survey were significantly lower than during the rest of the survey. At the end of the survey, TA_{35} values within sea-ice brine converged toward the values observed in seawater.

DMS—The largest changes and the highest concentrations of DMS were observed in the platelet ice-like layer, where concentrations ranged from 4 nmol L^{-1} up to 74 nmol L^{-1} (Fig. 5). At sta. C, DMS concentrations in brines and the platelet ice-like layer converged toward a value of 60 nmol L^{-1}, while values observed in the underlying water ranged between 1 nmol L^{-1} and 3 nmol L^{-1} and peaked at 17 nmol L^{-1}. Values observed in seawater were in the lower end of the range of DMS concentration reported in Southern Ocean waters (e.g., Trevena and Jones, 2006). DMS concentrations in brines were fourfold higher than within sea ice. To our best knowledge, no DMS concentrations in sea-ice brine have been previously reported, but it has been repeatedly

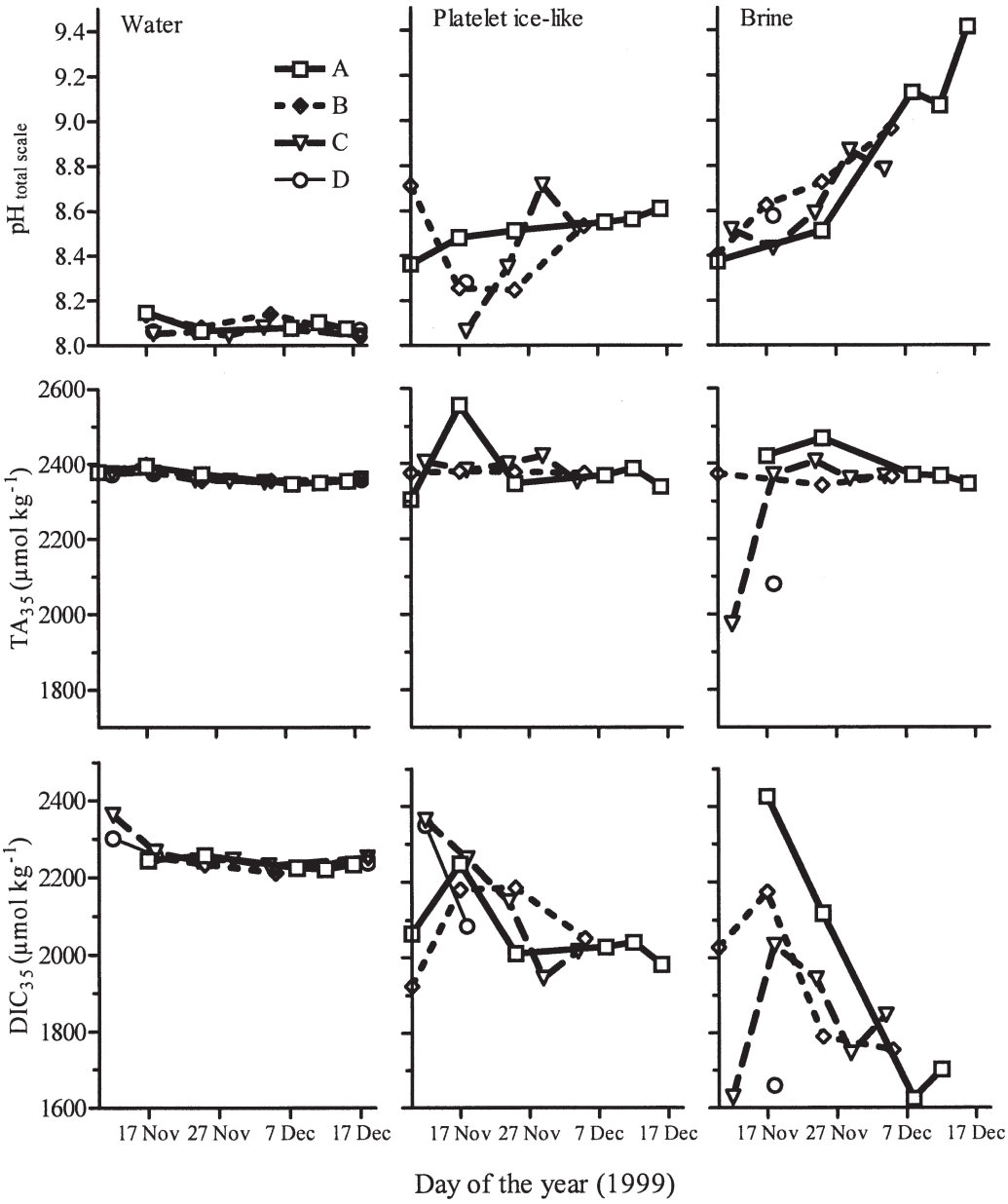

Fig. 6. Temporal variation of pH (on the total hydrogen ion scale), normalized total alkalinity (TA_{35}) and dissolved inorganic carbon (DIC_{35}) at a salinity of 35 within the underlying water, platelet ice-like layer, and brines at stations A, B, C, and D.

reported that values of DMS, DMSP, or DMS + DMSP in bulk ice can be one or two orders of magnitude higher in sea ice compared to the underlying water (Turner et al. 1995; Gambaro et al. 2004; Trevena and Jones 2006).

Discussion

The pCO_2 and O_2 dynamics in the underlying water—Undersaturation of O_2 (Hoppema et al. 1995; Gibson and Trull 1999) and oversaturation of CO_2 (Weiss 1987; Bakker et al. 1997; Gibson and Trull 1999) have been repeatedly reported beneath the ice cover in the Southern Ocean. The CO_2 oversaturation of seawater beneath ice as it was observed at the most-offshore stations C and D is generally thought to be related to winter hydrodynamics and/or organic matter decay. To our best knowledge, the only study of under-ice pCO_2 dynamics in nearshore waters surrounding Antarctica was carried out in Prydz Bay by Gibson and Trull (1999). Under-ice waters of Prydz Bay exhibited O_2 undersaturation, with values ranging from 80% to 85%; these values are consistent with our observations in Adélie Land. In Prydz Bay, waters remained CO_2 undersaturated almost throughout the year, but they evolved toward equilibrium and exhibited a marked decrease of pCO_2 before ice breakup. This decrease was ascribed to a sharp increase in Chl *a* concentration that had values up to 15.0 μg L^{-1} and was related primary production. In Adélie Land, with the exception of sta. A, late spring Chl *a* concentration remained below 1.0 μg L^{-1}. Before ice breakup, pCO_2 and O_2 concentra-

tions at the shallow stations A and B followed the pattern observed in Prydz Bay in November, with undersaturation of both O_2 and CO_2. However, CO_2 concentration remained close or above the equilibrium at the deepest stations C and D. Indeed, strong biological control of the pCO_2 seasonal changes in Prydz Bay is favored by its shallowness (bottom depth lower than 30 m at a distance of 3 km from the coast). In contrast, the coastal area of Adélie Land is characterized by a narrow shelf and marked topographic depressions. Bottom topography combined with strong katabatic winds favor Antarctic bottom water formation and deep mixing (Gordon and Tchernia 1972; Vaillancourt et al. 2003; Marsland et al. 2004), which may subsequently lead to significant upwelling of deep CO_2-rich waters. This may act to sustain CO_2 oversaturation in the Adélie Land deepest stations.

Values of pCO_2 reached a minimum at stations A, B, and C between 2 Dec and 6 Dec 99, just before ice breakup. At that time, brine temperature was above $-5°C$, i.e., the threshold for ice permeability (Golden et al. 1998). This allowed transfer of brines undersaturated in CO_2 from the ice to the underlying layer. This potentially contributed to the decrease of pCO_2 within underlying waters. In contrast, the general increase of pCO_2 at the very end of the survey at stations A, B, and C can be ascribed to wind-driven mixing of the surface layer with CO_2-rich deep waters, which would follow ice breakup because the water column would no longer be sheltered from wind stress.

The pCO_2 and O_2 dynamics within sea-ice brine—While Chl *a* concentration values remained below 2.0 $\mu g\ L^{-1}$ in brines, we observed a sustained increase of Chl *a* concentration in the bottom ice, from 1.0 $\mu g\ L^{-1}$ up to 164.0 $g\ L^{-1}$ of bulk ice during the survey. Such buildup of Chl *a* evidenced a large primary production that consumes CO_2, reduces both DIC_{35} and pCO_2, and produces O_2. We observed a large O_2 oversaturation in brines, up to 163%. Large O_2 oversaturations, up to 200%, have been previously observed within sea ice (Gleitz et al. 1995; Rysgaard et al. 2001).

At the start of the survey, we observed at stations C and D some TA_{35} values significantly lower than those of the underlying layer. Such patterns can be ascribed to $CaCO_3$ precipitation, which would have taken place prior to the sampling period, during autumn or winter. In 2001, mineral crystals were collected within ice in the same area that have been identified as $CaCO_3$ crystals (G.S. Dieckmann, pers. comm.). The dissolution of $CaCO_3$ crystals trapped in sea ice can lead to the increase of TA_{35} observed at stations C and D at the start of the survey. Subsequently, TA_{35} within–sea-ice brine converged with that of the underlying layer, likely due to the mixing of brines with the underlying water due to internal convection (Golden et al. 1998), which is likely to occur until the salinity of the brine becomes lower than the salinity of the underlying water (~34.7) (Fig. 3).

Assessment of the individual impact of main internal physical and biogeochemical processes on the brine pCO_2—We estimated the impact on the pCO_2 in brines of some physical and biogeochemical sea-ice processes that are potentially significant in spring, taking into account the observed increase of temperature and the subsequent decrease of salinity related to melting of ice crystals, together with $CaCO_3$ dissolution and organic matter production derived, respectively, from TA and O_2 changes.

Effect of increase of temperature and related decrease of salinity—The pCO_2 values predicted from the increase of temperature and related decrease of salinity due to melting of pure ice crystal ($pCO^{d}_{2(S,T)}$) were computed on day "d" using the CO_2 dissociation constants of Mehrbach et al. (1973) refitted by Dickson and Millero (1987) at salinity (S^d) and temperature (T^d) values of day "d", and from TA and DIC values (denoted as TA^{d}_{dil} and DIC^{d}_{dil}, respectively) expected from change of salinity related to the dilution with melted ice crystal according to:

$$TA^{d}_{dil} = TA^{d_0} \times \frac{S^d}{S^{d_0}} \quad (1)$$

and

$$DIC^{d}_{dil} = DIC^{d_0} \times \frac{S^d}{S^{d_0}}, \quad (2)$$

where TA^{d_0}, DIC^{d_0}, and S^{d_0} denote respectively TA, DIC, and salinity on the first day of the time-series d_0.

$CaCO_3$ dissolution effect—Dissolution of $CaCO_3$ within sea-ice brine is described by:

$$CaCO_3 + CO_2 + H_2O \Leftrightarrow Ca^{2+} + 2HCO_3^- . \quad (3)$$

Dissolution of 1 mole of $CaCO_3$ transfers CO_2 to the HCO_3^- pool, increasing DIC by 1 mole and TA by 2 moles. A simple approximation of the effect of $CaCO_3$ dissolution on DIC and TA (denoted as $\Delta DIC^{d}_{CaCO_3}$ and $\Delta TA^{d}_{CaCO_3}$) can be provided by assuming that the amount of $CaCO_3$ dissolved between day d_0 and day d is directly related to the change of TA normalized to the salinity of day d_0 according to:

$$\Delta TA^{d}_{CaCO_3} = TA^{d} - TA^{d_0} \times \frac{S^d}{S^{d_0}}, \quad (4)$$

where TA^d denotes TA on day d. $\Delta DIC^{d}_{CaCO_3}$ is related to $\Delta TA^{d}_{CaCO_3}$ according to

$$\Delta DIC^{d}_{CaCO_3} = 0.5 \times \Delta TA^{d}_{CaCO_3}. \quad (5)$$

Hence:

$$TA^{d}_{CaCO_3} = TA^{d_0} + \Delta TA^{d}_{CaCO_3} \quad (6)$$

and

$$DIC^{d}_{CaCO_3} = DIC^{d_0} + \Delta DIC^{d}_{CaCO_3}. \quad (7)$$

The pCO_2 expected from the dissolution of $CaCO_3$ ($pCO^{d}_{2(CaCO_3)}$) on day "d" was computed using the CO_2

dissociation constants of Mehrbach et al. (1973) refitted by Dickson and Millero (1987) from $TA^{d}_{CaCO_3}$ and $DIC^{d}_{CaCO_3}$ at the initial salinity S^{d_0} and temperature T^{d_0}.

Organic matter production—The assessment of organic matter production within sea-ice brine is difficult. We attempted to derive this production from the changes of O_2 concentration. Glud et al. (2002) reported complex O_2 dynamics in ice related to physical processes that can affect the computation. However, high concentration of O_2, DMS, and Chl *a* together with a dramatic decrease of CO_2 suggested that a strong biological activity developed in sea ice during the survey. Hence, a tight control of O_2 concentration by biological activity may therefore be expected in the brines. Thus, we assumed that during the survey, the evolution of the O_2 concentration provided a rough assessment of organic matter production by the sea-ice microbial communities. The Redfield reaction of organic matter production can be expressed as:

$$106CO_2 + 16NO_3^- + H_2PO_4^- + 17H^+ + 122H_2O \rightarrow (CH_2O)_{106}(NH_3)_{16}H_3PO_4 + 138O_2, \quad (8)$$

where 138 moles of O_2 are produced, while 106 moles of CO_2 are consumed. We estimated the production/removal of O_2, taking into account the O_2 dilution by melting ice crystals, according to:

$$\Delta O_2^d = [O_2]^d - [O_2]^{d_0} \times \frac{S^d}{S^{d_0}}, \quad (9)$$

where ΔO_2^d denotes the amount of O_2 produced/removed on day d since day d_0, and $[O_2]^d$ and $[O_2]^{d0}$ denote the concentration of O_2 on day d and d_0, respectively (given in μmol kg^{-1}).

DIC change associated with the production/removal of O_2 through organic matter production is given by:

$$\Delta DIC^d_{bio} = -\frac{106}{138}\Delta O_2^d, \quad (10)$$

where ΔDIC^d_{bio} denotes the DIC changes due to organic matter production by sea-ice microbial communities between days d and d_0. We used the Redfield ratio rather than the photosynthetic quotient (PQ) since we aimed to account for both primary production and respiration. The Redfield ratio of production of O_2 versus CO_2 consumption is about 1.30, which is close to average PQ observed in sea-ice communities of ~1.43 (Glud et al. 2002). According to Eq. 8, 1 mole of H^+ is consumed for each mole of NO_3^- or $H_2PO_4^-$ incorporated into organic matter, increasing TA by 1 mole.

We estimated the change of TA between day d and d_0, denoted as ΔTA^d_{bio}, due to organic matter production, according to:

$$\Delta TA^d_{bio} = -\frac{17}{106}\Delta DIC^d_{bio}. \quad (11)$$

We then derived the values of DIC and TA expected on day d from the production of organic matter according to:

$$TA^d_{bio} = TA^{d_0} + \Delta TA^d_{bio} \quad (12)$$

and

$$DIC^d_{bio} = DIC^{d_0} + \Delta DIC^d_{bio}. \quad (13)$$

We computed pCO_2 expected from organic matter production, denoted as $pCO^d_{2(bio)}$, on day d from TA^d_{bio} and DIC^d_{bio} at the initial salinity S^{d_0} and temperature T^{d_0}, using the CO_2 dissociation constants of Mehrbach et al. (1973) refitted by Dickson and Millero (1987). Finally, we computed TA and DIC derived from the sum of the three processes, respectively, TA^d_{all} and DIC^d_{all}, according to:

$$TA^d_{all} = TA^{d_0} + \Delta TA^d_{dil} + \Delta TA^d_{CaCO_3} + \Delta TA^d_{bio} \quad (14)$$

and

$$DIC^d_{all} = DIC^{d_0} + \Delta DIC^d_{dil} + \Delta DIC^d_{CaCO_3} + \Delta DIC^d_{bio}. \quad (15)$$

We computed $pCO^d_{2(all)}$ from TA^d_{all} and DIC^d_{all} at the temperature T^d and salinity S^d using the CO_2 dissociation constants of Mehrbach et al. (1973) refitted by Dickson and Millero (1987). Results from these computations at stations A, B, and C are shown in Fig. 7, together with the observed pCO_2 values.

The three processes reduce pCO_2. The temperature increase of ice brine from −5.7°C to −1.1°C before ice breakup drove the melting of ice crystals and subsequent salinity decrease from 90 to 24. This dilution decreased drastically both DIC and TA and led to a large pCO_2 drawdown (Fig. 7). The effect of dilution largely outweighed the increase of pCO_2 related to the increase of temperature, and this explains a large part of the pCO_2 decrease observed at the three stations. Organic matter production led to significant changes of pCO_2 at the three stations. At sta. A, the magnitude of pCO_2 changes due to organic matter production was similar to those related to dilution and $CaCO_3$ dissolution. The effect of $CaCO_3$ dissolution was also significant, but was only detected at the start of the experiment under relatively cold conditions, for brine temperatures below −4.5°C.

These computations address only the gases dissolved in brines and do not account for the amount of O_2 and CO_2 potentially trapped in bubbles. For instance, part of the O_2 generated by organic matter formation can accumulate in bubbles and is not accounted for in the estimate of organic matter production, while part of the CO_2 generated as a byproduct of winter $CaCO_3$ formation can also be trapped in bubbles (Killawee et al. 1998). The Redfield ratios are very likely affected by numerous processes, and O_2 dynamics are complex and not driven solely by biological processes (Glud et al. 2002). In addition, sea-ice thermodynamic constants used in dissolved inorganic calculations need to be formally validated. Also, potential effects of brine transport were not accounted in the mass balance, and precipitation and dissolution of $CaCO_3$

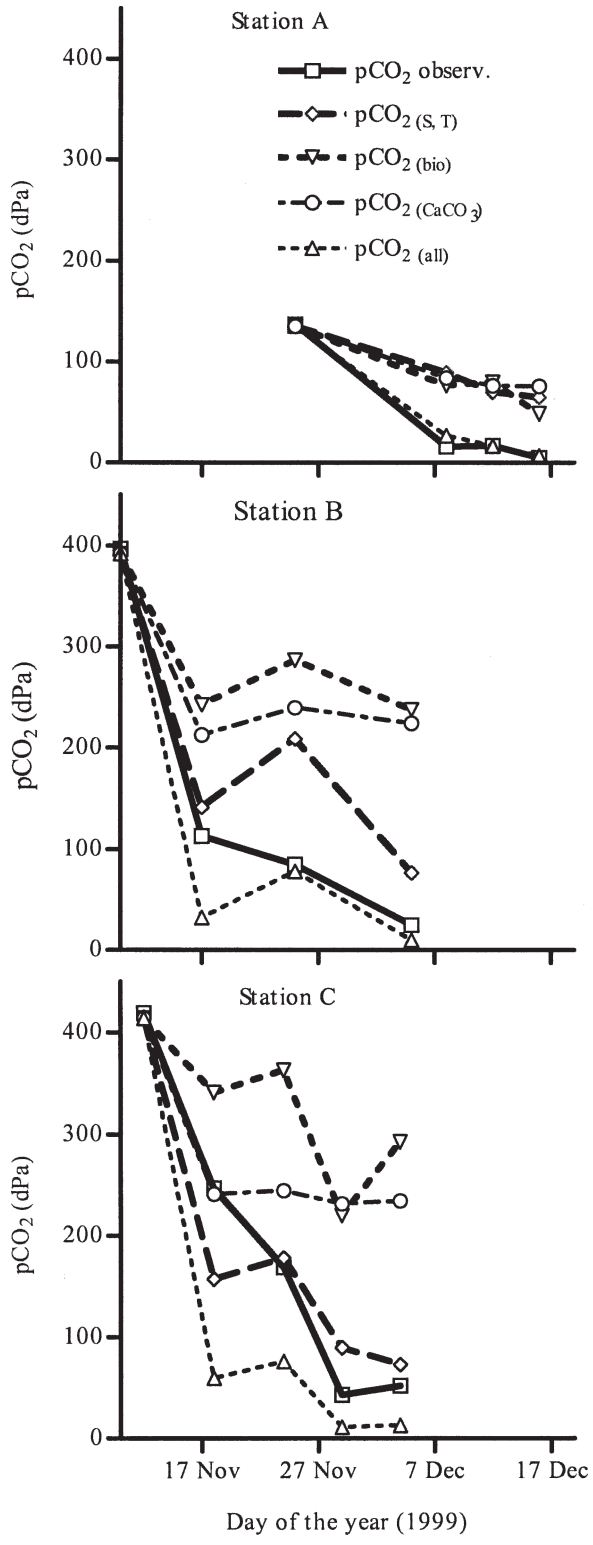

Fig. 7. Observed and computed partial pressure of CO_2 (pCO_2) at stations A, B, and C. Observed pCO_2 is indicated by a solid line with squares; pCO_2 computed from temperature and salinity changes ($pCO_{2(S,\ T)}$) is indicated by a dashed line with diamonds; pCO_2 computed from primary production derived from changes ($pCO_{2(bio)}$) is indicated by a dashed line with triangles down; pCO_2 computed from $CaCO_3$ dissolution derived from total alkalinity changes ($pCO_{2(CaCO3)}$) is indicated by a dot-dash line with circles; pCO_2 computed from all three processes ($pCO_{2(all)}$) is indicated by a dotted line with triangles up. Due to the poor reliability or lack of salinity measurements in brines on 10 Dec 99 at sta. A, simulations at this station were made from 25 Dec 99 onward. Horizontal dotted line corresponds to atmospheric pCO_2.

require further investigations. Finally, stations C and D showed a predicted pCO_2 decrease stronger than the observations (Fig. 7). This discrepancy might be ascribed to the mixing of brines with CO_2-oversaturated underlying water and/or CO_2 transfer from the atmosphere to the ice. During the survey, since the temperature of the ice brine was above $-5.0^{\circ}C$, the ice was permeable to both gases and liquids (Gosink et al. 1976; Golden et al. 1998), allowing both gas exchanges with the atmosphere and internal convection for brines with salinities above seawater salinity. Both processes act to maintain pCO_2 close to or above saturation and are not accounted for in our assessment. Hence, the difference between the observed and simulated pCO_2 signals might correspond to the CO_2 transfer from the neighboring environments toward the ice, which would then appear to act as a sink of CO_2 for the underlying water and/or the atmosphere.

Despite these uncertainties, the sum of changes of pCO_2 inferred from the three processes ($pCO^{d}_{2(all)}$) is quite consistent with the observed decrease of pCO_2. This suggests that we correctly identified three of the main biogeochemical processes driving pCO_2 dynamics during late spring within fast sea ice. Each process plays a significant role in the drastic spring decrease of pCO_2 in brines of land-fast ice. We acknowledge that during other seasons and in different ice types, CO_2 and the carbonate system could behave differently due to additional biogeochemical processes.

DMS dynamics—DMS concentrations in the underlying water layer were significantly lower than in sea ice from the very start of the experiment. Taking into account the low and constant Chl *a* concentration in seawater, the peak of DMS concentrations in seawater may be due to the input from sea ice rather than in situ production, as has been previously suggested (e.g., DiTullio et al. 1998; Trevena and Jones 2006). As mentioned above, brine temperature was above $-5.0^{\circ}C$ during most of the time, and brine salinity was above the salinity of the underlying water, thus internal convection likely drove the transport of DMSP and DMS from the ice brine to the underlying water.

We observed a threefold increase of DMS within sea-ice brine, and this was slightly enhanced in the platelet ice-like layer. This drastic increase of DMS production was inversely related to the decrease in salinity. The release of DMSP by healthy algal cells may occur in response to decreasing salinity (Stefels and Dijkhuizen 1996) during sea-ice melting in response to rapidly decreasing osmotic conditions, considering that DMSP acts as an osmolyte

(Dickson and Kirst 1986), or due to the increase of grazing activity subsequent to the widening of brine channels (Archer et al. 1996). As mentioned above, the decrease of salinity was also associated with drastic CO_2 drawdown and O_2 increase. Sunda et al. (2002) suggested that DMSP and DMS, by scavenging hydroxyl radicals and other reactive O_2 species, may serve as antioxidants that protect the cells in case of oxidative stress, which can include low CO_2 and high O_2 concentrations. This is supported by recent work of McMinn et al. (2005), which reported that the growth and photosynthesis of sea-ice algae communities are adversely affected by increasing external O_2 concentrations. These authors showed that ice algae are submitted to an oxic stress thought to be due to the occurrence of toxic O_2 species in high-O_2 conditions encountered in sea ice. An alternative explanation for the decrease of sea-ice algae growth with O_2 increase is the competition between carboxylase and oxygenase reactions at the site of ribulose-1,5-carboxylase/oxygenase. The relative rates of both reactions depend on the concentrations of the two gases, which are anticorrelated during sea-ice melting and reach extreme values that potentially favor the release of DMS. On the whole, from this study, it is not possible to decipher what is the main factor leading to the rapid release of DMS during sea-ice melting, but it is worth noting that the decrease of salinity led to uncommon low CO_2–high O_2 conditions that potentially favor the release of DMS.

The potentially significant flux of DMS from surface waters to the atmosphere related to sea-ice melting has already been pointed out by several authors. Levasseur et al. (1994) suggested that the release following ice melting of sea-ice DMSP within seawater could produce a one day pulse of DMS flux ten times higher than the average summer flux. In the same way, Trevena and Jones et al. (2006) suggested that the release of DMSP and DMS during sea-ice melting may result in "hot spots" of seawater DMS with concentrations of the order of 100 nmol L^{-1}. However, in the light of the growing body of evidence that CO_2 fluxes occur at the air–sea-ice interface, we surmise that as sea ice becomes permeable and allows direct gas transfer from the ice to the atmosphere, DMS might also escape from the ice directly to the atmosphere. Such transfer may be potentially significant taking into account the high DMS content of sea-ice brine. Thereafter, sea ice–related DMS release to the atmosphere may not be restricted to transient (Levasseur et al. 1994) and sparse (Trevena and Jones 2006) air-sea fluxes following sea-ice melting, and further studies of sea ice–related DMS emissions to the atmosphere should investigate potentially long-lasting air-ice transfer.

Platelet ice-like layer—The pCO_2, O_2, DIC_{35}, and DMS dynamics within the platelet ice-like layer mimicked patterns observed within brines. However, the magnitude of changes of O_2, pCO_2, and DIC_{35} was lower in the platelet ice-like layer than in the brines. This should be ascribed to both mixing with the underlying water and lower Chl *a* concentrations. With the exception of one measurement, TA_{35} remained constant throughout the survey, indicating that no dissolution of $CaCO_3$ took place within this layer. This suggests that either $CaCO_3$ dissolution occurred prior to the survey or that in the warmer and less saline conditions (salinity ranged from 29 to 41 during the survey) of the platelet ice-like layer, $CaCO_3$ precipitation did not occur. Finally, the few DMS measurements available indicated that DMS concentration was higher within the platelet ice-like layer compared to the brine and underlying water. This may have been due to an enhanced grazing pressure within the platelet ice-like layer, which is more accessible to grazers than the plain ice cover.

Biogases (CO_2, O_2, and DMS) exhibited strong dynamics within land-fast sea ice prior to ice breakup. Elevated O_2 and DMS concentrations were due to high sea-ice algae abundance and related primary production, which also decreased pCO_2. Other physical and biogeochemical processes, namely dilution of brines by melting ice crystals and $CaCO_3$ dissolution, also played a significant role in pCO_2, DIC, and TA dynamics. The pCO_2 values expected from salinity, temperature, O_2, and TA changes were lower than the observations prior to ice breakup, indicating the occurrence of an additional source of CO_2. This source can be ascribed to the transfer of CO_2 from neighbouring environments, i.e., the underlying water and/or the atmosphere, toward sea ice, suggesting that sea-ice cover acts as a CO_2 sink for one or both neighbouring environments. In parallel, high DMS concentrations encountered within sea-ice brine showed that sea ice could potentially act as a source of DMS for these neighbouring environments. According to salinity and temperature conditions, the sea-ice cover was permeable to gases and liquids, potentially allowing exchanges with the atmosphere. Although no measurements of DMS and CO_2 fluxes at the ice interfaces were carried out during the experiment, our data set indicates that spring land-fast sea ice can potentially act as a sink of CO_2 and as a source of DMS to the atmosphere.

References

Anderson, L. G., and E. P. Jones. 1985. Measurements of total alkalinity, calcium and sulfate in natural sea ice. J. Geophys. Res. **90:** 9194–9198.

Arar, E. J., and G. B. Collins. 1997. Method 445.0: *In vitro* determination of chlorophyll *a* and pheophytin *a* in marine and freshwater phytoplankton by fluorescence., National Exposure Research Laboratory, Office of Research and Development, U.S. Environmental Protection Agency.

Archer, S. D., R. J. G. Leakey, P. H. Burkill, M. A. Sleigh, and C. J. Appleby. 1996. Microbial ecology of sea ice at a coastal Antarctic site: Community composition, biomass and temporal change. Mar. Ecol. Prog. Ser. **135:** 179–195.

Arrigo, K. R., and D. N. Thomas. 2004. Large scale importance of sea ice biology in the Southern Ocean. Antarct. Sci. **16:** 471–486.

Bakker, D. C. E., H. J. W. de Baar, and U. V. Bathmann. 1997. Changes of carbon dioxide in surface waters during spring in the Southern Ocean. Deep-Sea Res. I **44:** 91–127.

DELILLE, B. 2006. Inorganic carbon dynamics and air-ice-sea CO_2 fluxes in the open and coastal waters of the Southern Ocean. Ph.D. thesis, Univ. of Liège.

DICKSON, A. G., AND F. J. MILLERO. 1987. A comparison of the equilibrium constants for the dissociation of carbonic acid in seawater media. Deep-Sea Res. I **34:** 1733–1743.

DICKSON, D. M. J., AND G. O. KIRST. 1986. The role of DMSP, glycine betaine and hoarine in the osmoacclimation of *Platymonas subcordiformis*. Planta **167:** 536–543.

DITULLIO, G., D. L. GARRISON, AND S. MATHOT. 1998. Dimethylsulfoniopropionate in sea ice algae from the Ross Sea Polynya, p. 139–146. *In* M. Lizotte and K. Arrigo [eds.], Antarctic sea ice biological processes, interactions and variability. American Geophysical Union.

DOE (DEPARTMENT OF ENERGY). 1994. Handbook of methods for the analysis of the various parameters of the carbon dioxide system in sea water. DOE.

FIALA, M., H. KUOSA, E. E. KOPCZYNSKA, L. ORIOL, AND D. DELILLE. 2006. Spatial and seasonal heterogeneity of sea ice microbial communities in the first-year ice of Terre Adélie area (Antarctica). Aquat. Microb. Ecol. **43:** 95–106.

GAMBARO, A., I. MORET, R. PIAZZA, C. ANDREOLI, E. DA RIN, G. CAPODAGLIO, C. BARBANTE, AND P. CESCON. 2004. Temporal evolution of DMS and DMSP in Antarctic coastal sea water. Int. J. Environ. Anal. Chem. **84:** 401–412.

GIBSON, J. A. E., AND T. W. TRULL. 1999. Annual cycle of fCO_2 under sea-ice and in open water in Prydz Bay, East Antarctica. Mar. Chem. **66:** 187–200.

GLEITZ, M., M. R. VONDERLOEFF, D. N. THOMAS, G. S. DIECKMANN, AND F. J. MILLERO. 1995. Comparison of summer and winter in organic carbon, oxygen and nutrient concentrations in Antarctic sea ice brine. Mar. Chem. **51:** 81–91.

GLUD, R. N., S. RYSGAARD, AND M. KUHL. 2002. A laboratory study on O_2 dynamics and photosynthesis in ice algal communities: Quantification by microsensors,O_2 exchange rates, C-14 incubations and a PAM fluorometer. Aquat. Microb. Ecol. **27:** 301–311.

GOLDEN, K. M., S. F. ACKLEY, AND V. I. LYTLE. 1998. The percolation phase transition in sea ice. Science **282:** 2238–2241.

GORDON, A. L., AND P. TCHERNIA. 1972. Waters of the continental margin off Adélie coast, Antarctica, p. 59–69. *In* D. E. Hayes [ed.], Antarctic Oceanology 2: The Australian-New Zealand sector. American Geophysical Union.

GOSINK, T. A., J. G. PEARSON, AND J. J. KELLEY. 1976. Gas movement through sea ice. Nature **263:** 41–42.

HOPPEMA, M., E. FAHRBACH, M. SCHRÖDER, A. WISTOTZKI, AND H. J. W. DE BAAR. 1995. Winter-summer differences of carbon dioxide and oxygen in the Weddell Sea surface layer. Mar. Chem. **51:** 177–192.

KILLAWEE, J. A., I. J. FAIRCHILD, J.-L. TISON, L. JANSSENS, AND R. LORRAIN. 1998. Segregation of solutes and gases in experimental freezing of dilute solutions: Implications for natural glacial systems. Geochim. Cosmochim. Ac. **62:** 3637–3655.

KIRST, G. O., C. THIEL, H. WOLFF, J. NOTHNAGEL, M. WANZEK, AND R. ULMKE. 1991. Dimethylsulfoniopropionate (DMSP) in ice-algae and its possible biological role. Mar. Chem. **35:** 381–388.

LEVASSEUR, M., M. GOSSELIN, AND S. MICHAUD. 1994. A new source of dimethylsulfide (DMS) for the arctic atmosphere-ice diatoms. Mar. Biol. **121:** 381–387.

MARION, G. M. 2001. Carbonate mineral solubility at low temperatures in the Na-K-Mg-Ca-H-Cl-SO_4-OH-HCO_3-CO_3-CO_2-H_2O system. Geochim. Cosmochim. Ac. **65:** 1883–1896.

MARSLAND, S. J., N. L. BINDOFF, G. D. WILLIAMS, AND W. F. BUDD. 2004. Modeling water mass formation in the Mertz Glacier Polynya and Adélie Depression, East Antarctica. J. Geophys. Res. **109**, C11003, doi: 10.1029/2004JC002441.

MCMINN, A., A. PANKOWSKI, AND T. DELFATTI. 2005. Effect of hyperoxia on the growth and photosynthesis of polar sea ice microalgae. J. Phycol. **41:** 732–741.

MEHRBACH, C., C. H. CULBERSON, J. E. HAWLEY, AND R. M. PYTKOWICZ. 1973. Measurements of the apparent dissociation constants of carbonic acid in seawater at atmospheric pressure. Limnol. Oceanogr. **18:** 897–907.

MILLERO, F. J., D. PIERROT, K. LEE, R. WANNINKHOF, R. FEELY, C. L. SABINE, R. M. KEY, AND T. TAKAHASHI. 2002. Dissociation constants for carbonic acid determined from field measurements. Deep-Sea Res. I **49:** 1705–1723.

NGUYEN, B. C., N. MIHALOPOULOS, AND S. BELVISO. 1990. Seasonal variation of atmospheric dimethylsulfide at Amsterdam Island in the Southern Indian Ocean. J. Atmos. Chem. **11:** 123–141.

PAPADIMITRIOU, S., H. KENNEDY, G. KATTNER, G. S. DIECKMANN, AND D. N. THOMAS. 2004. Experimental evidence for carbonate precipitation and CO_2 degassing during sea ice formation. Geochim. Cosmochim. Acta **68:** 1749–1761.

RIAUX-GOBIN, C., P. TREGUER, G. DIECKMANN, E. MARIA, G. VETION, AND M. POULIN. 2005. Land-fast ice off Adélie Land (Antarctica): Short-term variations in nutrients and chlorophyll just before ice break-up. J. Mar. Sys. **55:** 235–248.

RYSGAARD, S., R. GLUD, M. K. SEJR, J. BENDTSEN, AND P. B. CHRISTENSEN. 2007. Inorganic carbon transport during sea ice growth and decay: A carbon pump in polar seas. J. Geophys. Res. **112**, C03016, doi: 10.1029/2006JC003572.

———, M. KUHL, R. N. GLUD, AND J. W. HANSEN. 2001. Biomass, production and horizontal patchiness of sea ice algae in a high-Arctic fjord (Young Sound, NE Greenland). Mar. Ecol. Prog. Ser. **223:** 15–26.

SEMILETOV, I., A. MAKSHTAS, S. I. AKASOFU, AND E. L. ANDREAS. 2004. Atmospheric CO_2 balance: The role of Arctic sea ice. Geophys. Res. Lett. **31**, L05121, doi: 10.1029/2003GL017996.

STEFELS, J. 2000. Physiological aspects of the production and conversion of DMSP in marine algae and higher plants. J. Sea Res. **43:** 183–197.

———, AND L. DIJKHUIZEN. 1996. Characteristics of DMSP-lyase in *Phaeocystis* sp. (Prymnesiophyceae). Mar. Ecol. Prog. Ser. **131:** 307–313.

SUNDA, W., D. J. KIEBER, R. P. KIENE, AND S. HUNTSMAN. 2002. An antioxidant function for DMSP and DMS in marine algae. Nature **418:** 317–320.

THOMAS, D. N., AND G. S. DIECKMANN. 2002. Biogeochemistry of Antarctic sea ice. Oceanogr. Mar. Biol. **40:** 143–169.

TREVENA, A. J., AND G. B. JONES. 2006. Dimethylsulphide and dimethylsulphoniopropionate in Antarctic sea ice and their release during sea ice melting. Mar. Chem. **98:** 210–222.

———, G. B. JONES, S. W. WRIGHT, AND R. L. VAN DEN ENDEN. 2003. Profiles of dimethylsulphoniopropionate (DMSP), algal pigments, nutrients, and salinity in the fast ice of Prydz Bay, Antarctica. J. Geophys. Res. **108**, C53145, doi: 10.1029/2002JC001369.

TURNER, S. M., P. D. NIGHTINGALE, W. BROADGATE, AND P. S. LISS. 1995. The distribution of dimethylsulphide and dimethylsulphoniopropionate in Antarctic waters and sea ice. Deep-Sea Res. II **42:** 1059–1080.

VAILLANCOURT, R. D., R. N. SAMBROTTO, S. GREEN, AND A. MATSUDA. 2003. Phytoplankton biomass and photosynthetic competency in the summertime Mertz Glacier region of East Antarctica. Deep-Sea Res. II **50:** 1415–1440.

Weiss, R. F. 1987. Winter Weddell Sea Project 1986: Trace gas studies during legs ANT V/2 and ANT V/3 of Polarstern. Antarct. J. U.S. **22:** 99–100.

Zemmelink, H. J., B. Delille, J.-L. Tison, E. J. Hintsa, L. Houghton, and J. W. H. Dacey. 2006. CO_2 deposition over the multiyear ice of the western Weddell Sea. Geophys. Res. Lett. **33**, L13606, doi: 10.1029/2006GL026320.

———, L. Houghton, J. W. H. Dacey, A. P. Worby, and P. S. Liss. 2005. Emission of dimethylsulfide from Weddell Sea leads. Geophys. Res. Lett. **32**, L23610, doi: 10.1029/2005GL024242.

Received: 24 May 2006
Accepted: 7 December 2006
Amended: 13 February 2007